Bosonic fractional Chern insulating state at integer fillings in a multiband system

Wei-Wei Luo,[1] Ai-Lei He,[2] Yi-Fei Wang,[3] Yuan Zhou,[1,4,*] and Chang-De Gong[3,1]

[1]*National Laboratory of Solid State Microstructures and Department of Physics, Nanjing University, Nanjing 210093, China*

[2]*Institute for Advanced Study, Tsinghua University, Beijing 100084, China*

[3]*Center for Statistical and Theoretical Condensed Matter Physics, and Department of Physics, Zhejiang Normal University, Jinhua 321004, China*

[4]*Department of Mathematics and Physics, Xinjiang Teacher's College, Urumqi 830043, China*

(Received 9 April 2021; accepted 8 September 2021; published 15 September 2021)

The integer quantum Hall state occurs when Landau levels are fully occupied by fermions, while the fractional quantum Hall state usually emerges when the Landau level is partially filled by strongly correlated fermions or bosons. Here, we report two fractional Chern insulating states of hard-core bosons in a multiband lattice model hosting topological flat bands with a high Chern number. The previously proposed $\nu = 1/3$ fractional Chern insulating state inherited from the high Chern number $C = 2$ of the lowest topological flat band is revisited by the infinite density matrix renormalization group algorithm. In particular, we numerically identify a bosonic 1/2-Laughlin-like fractional Chern insulating state at the integer fillings. We show two lower topological flat bands jointly generate an effective $C = 1$ Chern band with half filling. Furthermore, we find a strictly particle-hole-like symmetry between the ν and $3 - \nu$ filling in our model. These findings extend our understanding of quantum Hall states and offer a route to realize fractional states in the system with multibands and high Chern numbers.

DOI: 10.1103/PhysRevB.104.115126

I. INTRODUCTION

The emergence of topological state and topological order opens a window to classify phases of matter beyond Landau's symmetry-breaking paradigm [1]. The precise quantization of Hall conductivity $\sigma_{xy} = C\frac{e^2}{h}$, with C a topological invariant Chern number, appears when the Landau levels generated by the external magnetic field are fully filled. In contrast, the fractional quantum Hall state is observed when the strongly interacting electrons partially fill a Landau level, whose topological order can be characterized by the ground-state degeneracy on a compact geometry and the gapless edge excitations described by the chiral Luttinger liquid [1,2]. Laughlin proposed a trial wave function that captures the essence of the fractional quantum Hall state, in which the quasiparticle excitations host the fractional charges and fractional braiding statistics [3]. Halperin further generalized the Laughlin state into the two-component system [noted as Halperin (*mmn*) state] to account for the spin or pseudospin degrees of freedom [4]. The lattice version of an integer quantum Hall state in the absence of the Landau level, also known as the Chern insulating state, was proposed on a honeycomb lattice model with staggered flux threading [5] and experimentally realized in solid-state materials [6] and cold atom systems [7]. Chern insulators, compared with their continuum counterpart, can survive in a less strict setup and host more exotic topological phases [8], and thus provide a promising application platform. Since the $C = 1$ Chern band can be adiabatically connected to the Landau level [9–11], the fractional quantum Hall effect was possible to be realized in lattice models. It was previously proposed for ultracold atoms confined in an optical lattice [12–14] in which the effective magnetic field was simulated by introducing oscillating quadrupole potential or lattice rotation. The proposal of a topological flat band (TFB) [15–17] in the absence of the external magnetic field opens a window to realize the fractional Chern insulator. Subsequently, a series of fractional Chern insulators were established in various lattice models hosting the $C = 1$ TFB [18–20].

Unlike the unit Chern number of the Landau level in the continuum limit, the lattice model can host high Chern numbers, such as in the Hofstadter model [21–23]. Similar bands with high Chern numbers can also be generated in the TFB lattice model. Initially, $C = 2$ TFBs were constructed in a dice lattice model [24] and three-band triangular lattice model [25], and the systematic approaches to generate TFBs with arbitrary Chern numbers were further proposed in multilayer systems [26] and multiorbital structures [27]. Although a $C > 1$ Chern band can be mapped to a C-component Landau level using hybrid Wannier states [28], these components are mutually entangled with each other, in contrast with the case in the usual Halperin state. A series of fermionic fractional Chern insulators at $\nu = 1/(2C + 1)$ filling were established numerically in TFB models with high Chern number C [25,29–31], which can be understood as the SU(C) color-entangled version of Halperin states [32,33]. On the other hand, the topological states in a bosonic system are much subtle. The bosonic fractional Chern insulators at $\nu = 1/(C + 1)$ filling were also proposed in the TFB models [25,29,34]. These incompressible states can also be understood by the concept of flux attachment in a lattice system [22,35], yielding a series of fractional Chern insulators at filling factors $\nu = r/(r|C| + 1)$ for bosons and $\nu = r/(2r|C| + 1)$ for fermions with r an integer [23]. The bosonic integer quantum Hall (BIQH) state,

*zhouyuan@nju.edu.cn

a topological phase protected by U(1) symmetry but in the absence of intrinsic topological order, was perceived in interacting two-component boson gases at the integer filling $\nu = 1 + 1$ [36–40]. Its existence was also predicted by the composite fermion theory at integer filling $\nu = 1$ of $|C| = 2$ band ($r = -1$) [23] and numerically confirmed in different lattice models [41–45].

So far, the topological nature of the Chern insulators follows a similar way established in the continuum limit with the Landau levels, i.e., the integer and fractional quantum Hall effect emerge at the integer and fractional filling. It is interesting to explore fractional Chern insulators with no analog in the continuum limit [22,46]. In this paper, combining the exact diagonalization (ED) and infinite density matrix renormalization group (iDMRG) algorithm, we study exotic fractional Chern insulators of hard-core bosons in a specific multiband model. The adopted triangular lattice model hosts two lower TFBs with respective Chern numbers $C = 2$, and -1. We numerically confirm the previously proposed $\nu = 1/3$ bosonic fractional Chern insulating (FCI) state. Its topological order is well characterized by the $\mathbf{K} = \left(\begin{smallmatrix} 2 & 1 \\ 1 & 2 \end{smallmatrix}\right)$-matrix, i.e., a color-entangled $\frac{1}{3}$-FCI state with the two components originating from the high Chern number $C = 2$ of the lowest TFB. More importantly, an unexpected bosonic FCI state, rather than the BIQH state, is observed at integer fillings $\nu = 1$ and $\nu = 2$. The twofold ground-state degeneracy and the exact fractional-1/2 charge pumping, as well as the level counting of the low-lying entanglement spectrum, evidence the emergence of a $\nu = 1/2$ Laughlin-like FCI state. We identify that the two lower TFBs produce an effective $C = 1$ Chern band with half filling. In addition, we find a strict particle-hole-like symmetry between the ν and $3 - \nu$ filling inherited from the intrinsic time-reversal symmetry of the specific model.

II. MODEL AND METHOD

We consider loading hard-core bosons with U(1) charge conservation into a specific three-band triangular-lattice model proposed by one of our authors [25]:

$$H = \pm t \sum_{\langle ij \rangle} [b_i^\dagger b_j \exp(i\phi_{ij}) + \text{H.c.}] \pm t' \sum_{\langle\langle ij \rangle\rangle} [b_i^\dagger b_j \exp(i\phi_{ij}) + \text{H.c.}], \quad (1)$$

where $b_i^\dagger$ creates a hard-core boson at site i, $\langle \dots \rangle$ and $\langle\langle \dots \rangle\rangle$ denote the nearest-neighbor (NN) and the next-nearest-neighbor (NNN) pairs of sites with the specified phase factor denoted by the arrows (Fig. 1), respectively. Each unit cell (gray hexagon) contains three inequivalent sites and thus three single-particle bands are created. The flatness ratio and topological index of each band are parameter dependent (for more details, see Appendix A). Here we fix $t = 1$, $t' = 1/4$, and $\phi = \pi/3$ [25] unless specified, yielding $C = 2, -1, -1$ in each band (from bottom to top) and two lower flat bands with respective flatness ratios of about 15, 14, respectively. Those TFBs mimic the Landau levels in the continuum but with diverse Chern numbers. We, therefore construct a multiband model with high Chern numbers.

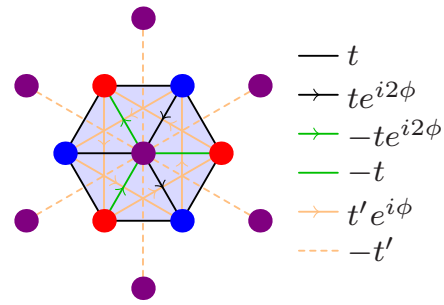

FIG. 1. Schematic structure of the adopted triangular lattice model. The unit cell is highlighted by a gray hexagon and the hopping process between the NN and NNN neighbors with specified gauges are given on the right-hand side.

Numerically, we employ the unbiased ED and iDMRG methods to study the topological order of potentially topological states. In the ED scheme, a finite system of $N_{\text{orb}} = N_x \times N_y$ unit cells (the total number of site $N_s = 3 \times N_x \times N_y$) with periodic boundary conditions in both directions is considered. The filling factor is defined as $\nu = N_b/N_{\text{orb}}$ with N_b the number of hard-core bosons loaded. Due to the translational symmetry, the many-body eigenstates can be labeled by the total momentum quantum number (k_x, k_y) in units of $(2\pi/N_x, 2\pi/N_y)$. To access larger system sizes and extend numerical evidence beyond the ED method, we also study the interacting system on an infinite cylinder (with finite width L_y) by iDMRG alogrithm [47,48]. This method allows us to directly simulate the charge pumping process [49–52] and conveniently explores the underlying topological order by the entanglement properties in the many-body ground state [53,54].

A. FCI state at $\nu = 1/3$

The $\nu = 1/3$ bosonic fractional Chern insulator had been previously studied by the ED method on a torus geometry [25,55]. The low-lying energy spectrum in Fig. 2(a) unambiguously shows that three quasidegenerate ground states, being robust against the boundary conditions, evolve into each other while being well separated from the higher excited states. By imposing the twisted boundary phases θ_x and θ_y in both directions, the Chern number of a many-body ground-state is given by $C = \frac{1}{2\pi} \int_0^{2\pi} \int_0^{2\pi} d\theta_x d\theta_y F(\theta_x, \theta_y)$, where $F(\theta_x, \theta_y) = \Im(\langle \partial_{\theta_x} \psi | \partial_{\theta_y} \psi \rangle - \langle \partial_{\theta_y} \psi | \partial_{\theta_x} \psi \rangle)$ is the gauge-invariant Berry curvature with ψ the ground-state wave functions [56]. The Berry curvature of the ground-state manifold [Fig. 2(b)] contributes a total Chern number $C = 2$. The topological order of the $\nu = 1/3$ FCI state can be well characterized by the $\mathbf{K}$ matrix in terms of Chern-Simons field theory [57,58]. Here, the ground-state degeneracy $d = \det \mathbf{K} = 3$ and the total Chern number $C = \sum_{i,j} (\mathbf{K}^{-1})_{ij} = 2$, yielding $\mathbf{K} = \left(\begin{smallmatrix} 2 & 1 \\ 1 & 2 \end{smallmatrix}\right)$. Alternatively, this $\nu = 1/3$ state is also predicted by composite fermion theory [23] at bosonic filling $\nu = r/(r|C| + 1)$ with $r = 1$, where one flux quantum is attached to each boson to form the weakly interacting composite fermion. An incompressible state is expected to form when they fully fill an integer number of Chern bands.

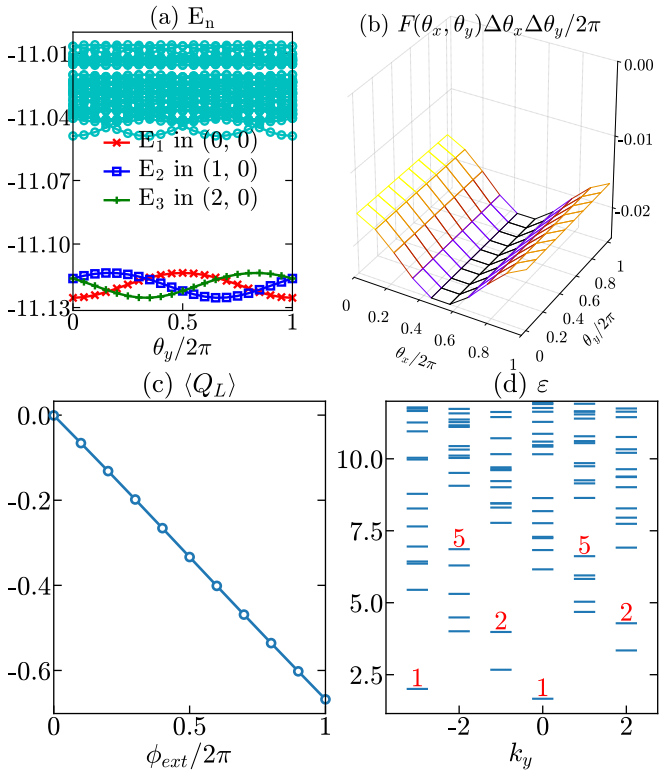

FIG. 2. $\nu = 1/3$ FCI state. (a) Spectral flow as a function of twist boundary phase θ_y. (b) Total Berry curvature of the three quasidegenerate ground states at 10×10 mesh points, which shares a total Chern number $C = 2$. (c) 2/3 charge pumping during the adiabatic flux quanta insertion. (d) Momentum-resolved entanglement spectrum revealing two branches of chiral edge modes, each with degeneracy pattern: 1, 2, 5. The lattice size $N_s = 3 \times 3 \times 5 = 45$ is used in ED calculation. The cylinder width $L_y = 6$ is adopted in iDMRG calculation.

To complement the ED results on a torus, we study the $\nu = 1/3$ case on a cylinder geometry using the iDMRG algorithm. The exact 2/3 charge pumping after a flux quanta threading [Fig. 2(c)] agrees with the Chern number calculation using the ED method [25], where each ground-state average contributes to a Chern number $C = 2/3$. Furthermore, two parallel propagating edge modes with the same level counting $(1, 2, 5, \cdots)$ are observed in the momentum-resolved entanglement spectrum of the ground state [Fig. 2(d)], in agreement with two positive eigenvalues in the **K**-matrix description and the low-lying structure of edge excitations in 1/3 FQH systems [53,59]. Therefore, the present state is a two-component fractional quantum Hall state, in which the two-component nature originates from the $C = 2$ Chern number of the lowest TFB. The exact equivalence between the two components render the bosonic FCI state a color-entangled $\frac{1}{3}$-FCI state [32,33,55], which differs from the general two-component $\nu = 1/3 + 1/3$ case discussed previously in the Bose gas with two spin states [38,60], though they share a similar topological order.

B. FCI state at $\nu = 1$

It is commonly accepted that the integer quantum Hall effect emerges when electrons fully fill the Landau levels. The BIQH, characterized by $\mathbf{K} = \left(\begin{smallmatrix} 0 & 1 \\ 1 & 0 \end{smallmatrix}\right)$, were predicted in the lowest Landau level filled with two-component interacting bosons at total filling $\nu = 1 + 1$ [36,37]. This state was also proposed in the Hofstadter model when the $C = 2$ Chern bands are fully occupied by the hard-core bosons [43]. It is thus interesting to explore the potential state in the current lattice model at integer filling.

We study the low-lying energy spectrum of different lattice sizes up to 36 sites with the ED scheme, which is almost the current computational limit (Hilbert space dimension reaches 10^8 for a single momentum sector). The twofold quasidegenerate ground states, separated from the excited states by a finite gap, emerge at the fixed momentum sector $(k_x, k_y) = (0, 0)$, irrespective of the lattice size [Fig. 3(a)]. The robustness of the ground-state manifold is also confirmed by the twisted boundary conditions $\theta_{x/y}$ [Fig. 3(b)], where the two states never mix with higher excited states. This agrees with the previous statistical rule in $C = 1$ TFB systems [19,20,25,61], where two ground states are predicted to emerge at (k_x, k_y) and $(k_x + N_b, k_y + N_b)$ mod (N_x, N_y) sector, respectively. In contrast, only a single ground state is observed in the $C = 2$ Hofstadter bands at $\nu = 1$ [43], in which a BIQH state is predicted. The FCI at integer filling $\nu = 1$ is further supported by the iDMRG results. The charge pumping after a flux quanta threading is exactly 1/2 [Fig. 3(d)]. This agrees with the existence of two degenerate ground states carrying a total Chern number $C = 1$. Moreover, only a single branch of the edge mode is observed in the momentum-resolved entanglement spectrum [Fig. 3(e)], in sharp contrast with the usual situation of two branches of edge modes in a $C = 2$ band. The corresponding counting sequence $(1, 1, 2, 3, 5, 7, \cdots)$ is consistent with that in a 1/2 Laughlin state. Therefore, we find a 1/2 Laughlin-like FCI state at the integer filling $\nu = 1$, rather than the expected BIQH state.

The confirmed evidence of 1/2 Laughlin-like fractional Chern insulator comes from the many-body Chern number of the ground-state wave function by integrating the Berry curvature in the first Brillouin zone. The discrete Berry curvatures [56] are relatively smooth [Fig. 3(c)]. Their summations yield a precisely quantized Chern number $C_{\text{tot}} = 1$ or, averagely, a $C = 1/2$ fractional Chern number for each ground state. This is in stark contrast to the FCI states reported at the bosonic $\nu = 1/3$ filling and the fermionic $\nu = 1/5$ filling in this model before [25] and the BIQH state reported in bosonic gases [36,37] and the Hofstadter band [43], where the ground-state manifold contributes to a total Chern number $C_{\text{tot}} = 2$. Considering the fact of two lower TFBs with $C = 2$ and $C = -1$ in our model, it is natural to believe that the hard-core bosons occupy the two lower TFBs simultaneously, which effectively generate a $C = 1$ topological band but with $\nu = 1/2$ filling. It was previously reported giving width to the Chern band with a high Chern number can help to stabilize a fractional Chern insulator [30]. Here, the two TFBs, instead of a high Chern number, play a similar role, which may be the reason why the 1/2 FCI state remains robust at the integer filling though the effective flatness ratio of the generated $|C| = 1$ Chern band is much reduced down to about 4 (details see Appendix A). The less strict condition for the fractional Chern insulator may provide a platform to realize the fractional quantum Hall state in multiband systems.

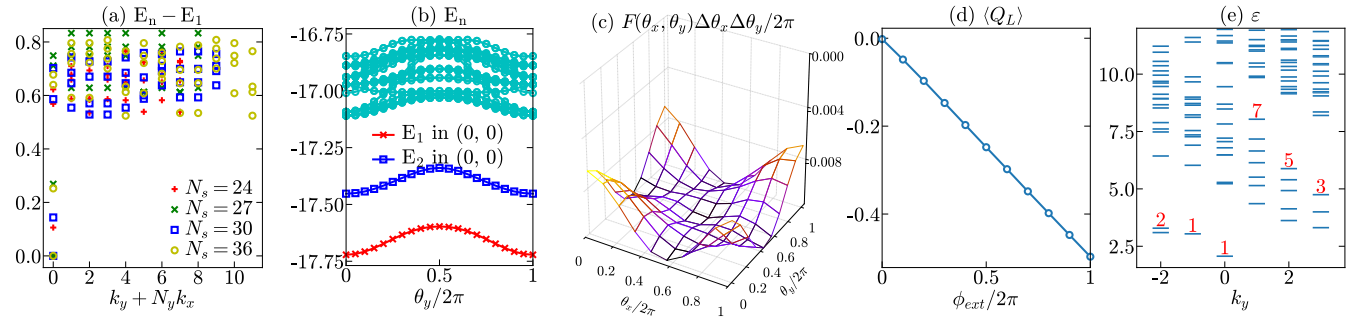

FIG. 3. $\nu = 1$ FCI state. (a) Low-lying energy spectrum for different lattice sizes. (b) Spectral flow as a function of twist boundary phase θ_y. (c) Total Berry curvature of the two ground states, which share a total Chern number $|C| = 1$. (d) 1/2 charge pumping during adiabatic flux quanta insertion. (e) Momentum-resolved entanglement spectrum revealing one branch of chiral edge mode, with degeneracy pattern: 1, 1, 2, 3, 5, 7. The lattice size $N_s = 3 \times 3 \times 3 = 27$ is used in ED calculation. The cylinder width $L_y = 6$ is adopted in iDMRG calculation.

C. Robustness of FCI state at $\nu = 1$

A similar band topology but in the absence of flat bands was previously constructed in a specific Hofstadter lattice model [31], where the BIQH state is predicted at integer filling with hard-core bosons [43]. It is therefore interesting to study whether the FCI state at integer filling turns into the BIQH state, or other competing order, when the flatness of TFBs is lowered. The flatness of TFBs is closely related to the NNN hopping integral t' (Appendix A). We show the low-energy many-body spectrum $E_n - E_1$ evolving with t' in Fig. 4(a) on a torus with fixed $N_s = 3 \times 3 \times 3 = 27$ sites. The twofold ground-state quasidegeneracy remains evident among $0.12 \leqslant t' \leqslant 0.4$, indicating the robustness of a FCI state at $\nu = 1$ filling in this region. When t' is reduced down to below 0.12, only a single ground state separated by excited states is observed. In contrast to BIQH, this is a trivial state with $C = 0$. Another phase transition is observed at $t' = 0.4$, where the underlying band topology changes (Appendix A). We do not find any signature of the BIQH state within the current setup.

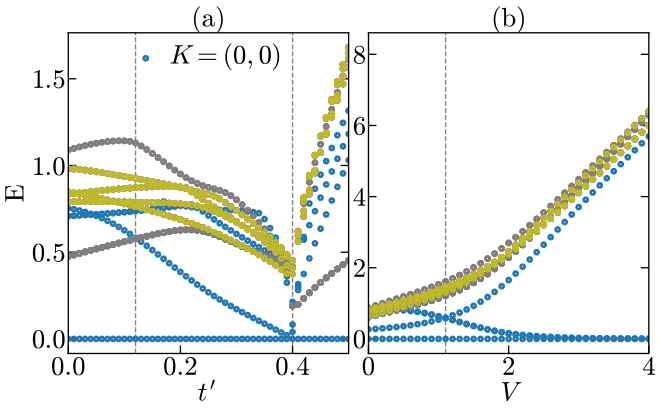

FIG. 4. Robustness of $\nu = 1$ FCI state. Evolution of low-lying energy spectrum versus NNN hopping strength t' (a) and NN interaction V (b). System size is $N_s = 3 \times 3 \times 3 = 27$. Colors label distinct momentum sectors, in particular, states at (0,0) momentum sector are colored blue. In (a), the $\nu = 1$ FCI state is dominated between $0.12 < t' < 0.4$, where the two ground states always share a Chern number $|C| = 1$. Beyond this region, two topologically trivial states emerge. In (b), a phase transition from the 1/2 Laughlin-like FCI state to the topologically trivial charge-density-wave state occurs at $V = 1.1$ at integer fillings $\nu = 1$.

On the other hand, the FCI state is often challenged by other conventional ordered states in strongly correlated systems [18], e.g., the charge-density-wave state may be favorable when long-range Coulomb interactions are taken into account [19,54]. We further discuss the role of NN Coulomb repulsion V [62] on the FCI state. In the large V limit, the loading bosons tend to occupy the NNN neighbors, i.e., the same sublattice, to lower energy contributed by the Coulomb repulsion. Figure 4(b) shows a phase transition occurring at $V_c \simeq 1.1$. The FCI state at the integer filling $\nu = 1$ is robust below V_c since the twofold quasidegeneracy remains. Above the critical V_c, a topologically trivial charge-density-wave state characterized by the threefold quasidegenerate ground state emerges, in agreement with the constructed three sublattices in our model.

D. Particle-hole symmetry

Since no band projection is performed here, we are able to study the system at higher fillings with $\nu > 1$. Given the unexpected FCI state at $\nu = 1$ filling, in which an effective $\frac{1}{2}$-filled Chern band with $C = 1$ is produced, is it possible that the BIQH state emerges when the two lower TFBs are fully occupied? Our numerical results on $\nu = 2$ filling show that the present bosonic system remains in the 1/2 Laughlin-like FCI state. We, therefore, establish a fractional Chern insulator at the integer fillings in our constructed bosonic lattice model. It should be emphasized that the energy spectrum at $\nu = 2$ filling is exactly the same as that at $\nu = 1$ filling. The charge pumping, and entanglement spectrum, except for a minus sign and the reversal propagating direction, respectively, are also the same (Appendix B). Similar behavior can be further observed at the filling of $\nu = \frac{1}{3}$ and $\nu = \frac{8}{3}$. It seems that there exists a particle-hole-like symmetry between ν and $3 - \nu$ filling in our adopted model. The particle-hole symmetry between the ν and $1 - \nu$ filling of fermions and between ν and $2 - \nu$ filling of two-component bosons in the quantum Hall state was previously reported when particles partially occupy

the lowest Landau level [40,63], where the particle-hole symmetry is preserved due to the perfectness of the Landau level. Here, no such symmetry explicitly exists as revealed by the band structure. Considering a particle-hole transformation $\mathcal{P}_{\rm ph}$ i.e., $b_i^\dagger \leftrightarrow b_i$, yielding $\mathcal{P}_{\rm ph} H(\phi)\mathcal{P}_{\rm ph}^{-1} = H(-\phi)$. We show that the only difference between ϕ and $-\phi$ is the reversed sign of the Chern number for each band. Therefore, an additional particle-hole-like symmetry between ν and $3-\nu$ filling exists in our constructed bosonic lattice model. Such symmetry originates from the intrinsic commute relation of bosons and the special time-reversal symmetry of the model Hamiltonian (for more details, see Appendix B). We emphasize that no particle-hole symmetry is presented in the corresponding fermionic system.

III. SUMMARY AND DISCUSSION

In summary, we study the FCI states of hard-core bosons on a specific three-band triangular lattice model possessing two lower TFBs with $C = 2$ and $C = -1$. Combining the ED and iDMRG algorithm, we characterize the underlying topological orders by ground-state degeneracy, low energy spectrum, and Chern number, together with charge pumping and entanglement spectrum. At $\nu = 1/3$ filling, a color-entangled $\frac{1}{3}$ FCI state is observed, in which two components come from the Chern number $C = 2$ of the lowest TFB. Particularly, instead of a BIQH state, we find a robust $1/2$ Laughlin-like FCI state at the integer fillings. The loading hard-core bosons simultaneously occupy the two lower TFBs, producing an effective $C = 1$ Chern band with $\nu = 1/2$ filling. In addition, a strict particle-hole-like symmetry between the ν and $3-\nu$ fillings, originating from the intrinsic commute relation of bosons and the time-reversal symmetry of the specific model, is revealed in the present lattice model. Our results demonstrate the rich family of topological states in lattice systems with high Chern number and multibands, and add the insight into the FCIs.

Further understanding the topological order of the present FCI state at integer fillings, especially constructing a model fractional state and performing the overlap with the ground-state wave function obtained by the ED method, is highly desirable. Exploring more exotic FCI states and potential relation to the generalized Pauli principle in the multiband system with nontrivial topology should be interesting for future study. Such multiband physics is neglected in most previous studies due to the simplified band projection. Whether the multiband-induced fractional Chern insulators can also be realized in the fermionic system is also interesting. Very recently, a direct transition between $\frac{1}{3}$ Laughlin state and Chern insulating state driven by the interaction was reported in the Harper-Hofstadter model loaded by fermions [64], where the lowest Landau level comprises multiple subbands. This may be the clue of the multiband and high Chern number induced fractional state at integer filling in fermionic systems.

The single-occupancy constraint of hard-core bosons may prevent the emergence of a BIQH state in the present lattice model. Whether the BIQH state will survive in this TFB model loaded by soft-core bosons, especially for intermediate interaction regime, is also an interesting problem worth delicate investigation. An initial study of three-body hard-core bosons with intermediate Hubbard interaction strength has not given any clue of the BIQH state. Since the computational effort to study the full phase diagram in the current TFB model with soft-core bosons are much larger than that of hard-core bosons, and more exotic non-Abelian FCI phases that occupy multiple Chern bands may also emerge, we will leave the numerically intensive problem to a detailed future work.

ACKNOWLEDGMENTS

We thank S.-L. Yu, W. Zhu, and T.-S. Zeng for helpful discussions. This work is supported by the National Natural Science Foundation of China Grants No. 12074175 and No. 11874325. Y.Z. and C.D.G. also acknowledge the Ministry of Science and Technology of China under Grant No. 2016YFA0300401. A.L.H. acknowledges the China Postdoctoral Science Foundation (No. 2020M680499).

APPENDIX A: SINGLE-PARTICLE ENERGY SPECTRUM

The adopted triangular lattice model loaded with the hard-core bosons has been schematically shown in the main text. The model Hamiltonian can be written as [25]

$$H = \pm t \sum_{\langle ij\rangle} [b_i^\dagger b_j \exp(i\phi_{ij}) + \text{H.c.}] \pm t' \sum_{\langle\langle ij\rangle\rangle} [b_i^\dagger b_j \exp(i\phi_{ij}) + \text{H.c.}]. \tag{A1}$$

Each unit cell comprises three inequivalent sites, which naturally produce three single particle bands. Only the NN and the NNN hopping process of the hard-core bosons are considered. It should be remembered that no on-site term exists in our model, which is crucial for the particle-hole-like symmetry existing in the present bosonic model as discussed below. In addition, we restrict our model in the canonical ensemble, which guarantees the particle number conservation. Even though no explicit interactions are considered, the model system remains strongly correlated due to the nature of hard-core boson.

The band topology of the present lattice model is parameter dependent. In Fig. 5, we show the band structure on a cylinder evolving with the next-NN hopping integral t' at fixed $\phi = \pi/3$. A topological phase transition occurs at $t_c' = 1/3$. Below t_c', the Chern number for the respective Chern band is $(2, -1, -1)$ (from bottom to top), while it turns out to be $(-4, 5, -1)$ for $t' > t_c'$. For large enough $t' > 1$, a topological phase with Chern number $(5, -4, -1)$ may also exist. We emphasize that a special time-reversal-like symmetry exists in the present model. The band structure remains unchanged except for the reversed Chern number for each band when $\phi \to -\phi$ but with the other parameters fixed. The chiral edge states shown in Fig. 5 reverse their propagating direction (not shown).

On the other hand, the flatness ratio of the respective topological band also varies with parameters as shown in Fig. 6. We define the flatness ratio of the respective lower topological band by Δ_i/W_i, where Δ_i, and W_i denotes the band gap above, and the bandwidth of, the selected ith band ($i = 1, 2$ from bottom to top), respectively. With fixed $\phi = \pi/3$, the flatness

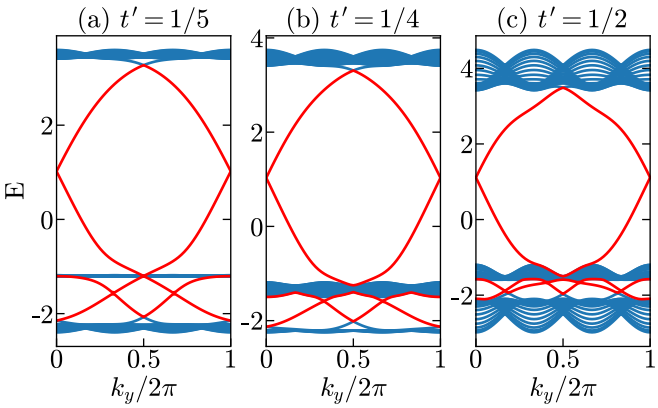

FIG. 5. Single-particle spectrum of the three-band triangular lattice model for different t' at fixed $\phi = \pi/3$. (a) and (b) The Chern numbers, from low to high energy bands, for $t' < 1/3$ topological phase is $(2, -1, -1)$. (c) Higher-Chern-number bands exists for $t' > 1/3$, which is $C = (-4, 5, -1)$ at $t' = 1/2$.

ratio of the lowest TFB reaches its maximum at $t' = \frac{1}{4}$. It decreases monotonically with enhanced or weakened t'. The flatness ratio of the middle TBF could be higher than 200 at $t' = \frac{1}{5}$. As mentioned in main text, the two lower TFBs jointly generate an effective $C = 1$ Chern band at integer fillings, which is the reason for the emergence of $\frac{1}{2}$ Laughlin-like FCI state at integer filling. We also show the flatness ratio of the generated effective $C = 1$ Chern band comprising two lower TFBs, defined as $R_T = \Delta_2/(W_1 + W_2 + \Delta_1)$. The flatness ratio of this Chern band in the region where the $\frac{1}{2}$ Laughlin-like FCI state at integer fillings is observed is relative high, but much reduced in comparison with that of the respective TFB. In this sense, the multiband physics provides the easy access to the FCI state.

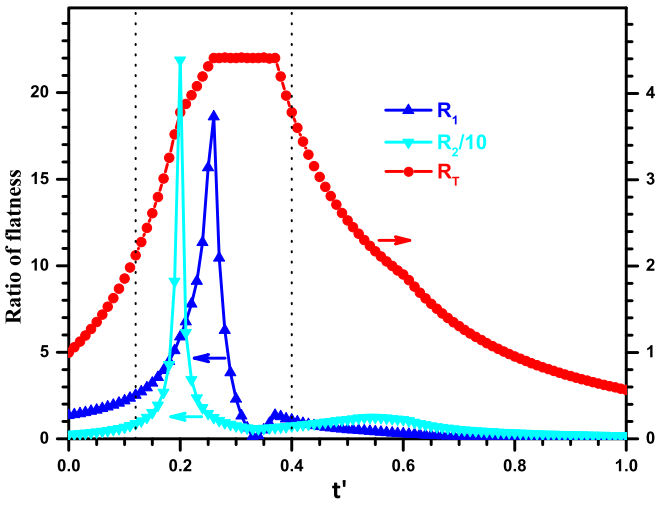

FIG. 6. t' dependence of the flatness ratio of the respective topological flat band, together with that of the generated $C = 1$ Chern band. The flatness ratio of the middle topological flat band is renormalized by a factor of 10. ϕ is fixed at $\pi/3$.

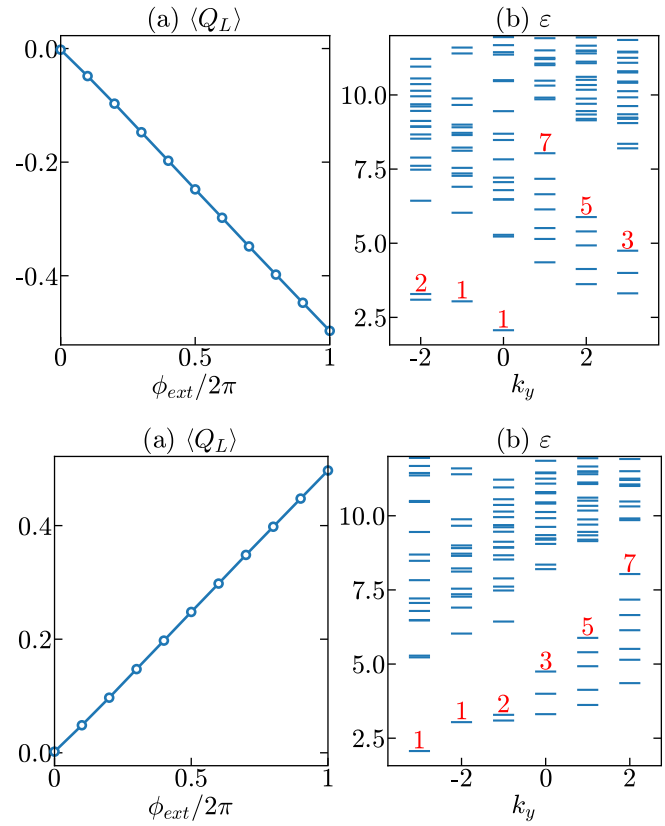

FIG. 7. $\nu = 1$ (top) and $\nu = 2$ (bottom) FCI states. (a) $1/2$ charge pumping after one flux insertion. (b) Momentum-resolved entanglement spectrum reveals one branch of chiral edge mode with degeneracy pattern: 1, 1, 2, 3, 5, 7,... The two FCI states are time-reversal counterparts of each other, where the charge pumping differs by a sign and edge mode differs by the propogating direction.

APPENDIX B: PARTICLE-HOLE-LIKE SYMMETRY

Obviously, the band structure in the above section shows no particle-hole symmetry for fermions. However, the situation in the bosonic system is significantly different from that in the fermionic system due to the intrinsic statistical law. In a hard-core bosonic system, we apply the particle-hole transformation $\mathcal{P}$, i.e., $b^\dagger \leftrightarrow b$, on Hamiltonian Eq. (A1), yielding

$$H = \pm t \sum_{\langle ij \rangle} [b_j b_i^\dagger \exp(i\phi_{ij}) + \text{H.c.}] \pm t' \sum_{\langle\langle ij \rangle\rangle} [b_j b_i^\dagger \exp(i\phi_{ij}) + \text{H.c.}]. \quad \text{(B1)}$$

Due to the commute relation between $[b_i, b_j^\dagger] = 0$, we have $\mathcal{P}H(\phi)\mathcal{P}^{-1} = H(-\phi)$. We have shown that the band structure remains unchanged except for the reversed Chern number for $\phi \to -\phi$. Therefore, the only change for the topological state is the reversed propagating direction, or *particle* to *hole*. Such particle-hole symmetry may be broken when the mass terms, i.e., $b_i^\dagger b_i$, are taken into account, by which $[b_i, b_i^\dagger] = 1$. Therefore, the particle-hole-like symmetry found in the present bosonic lattice model originates from the intrinsic commute relation of the bosons and the unique time-reversal

symmetry of the specific model. This symmetry is naturally absent in the fermionic system due to the anticommute relation of fermionic operators.

The particle-hole-like symmetry may be further understood by mapping the hard-core bosons onto the spin-$\frac{1}{2}$ quantum model. Using the Matsuda-Matsubara transformation, $b_i^\dagger \to S_i^+$, $b_i \to S_i^-$, and $n_i \to S_i^z + \frac{1}{2}$, the above Hamiltonian can be expressed as

$$H = \pm t \sum_{\langle ij \rangle} [S_i^+ S_j^- \exp(i\phi_{ij}) + \text{H.c.}] \pm t' \sum_{\langle\langle ij \rangle\rangle} [S_i^+ S_j^- \exp(i\phi_{ij}) + \text{H.c.}]. \quad \text{(B2)}$$

The particle-hole transformation in the bosonic model is same as the spin-flip process in spin model. In the absence of symmetry breaking term S_i^z, the above Hamiltonian after spin flip also results in $H(-\phi)$.

In Fig. 7, we plot the charge pumping and entanglement spectrum to show the particle-hole-like symmetry between $\nu = 1$ and $\nu = 2$, in which a 1/2 Laughlin-like FCI state is realized at integer fillings. The two cases are almost exactly the same, except for the charge (or hole) pumping process and reversal propagating direction. Similar behavior can be also found at the integer filling $\nu = 1/3$ and $\nu = 8/3$, where a color-entangled $\frac{1}{3}$ FCI state is observed.

[1] X. G. Wen, Topological orders in rigid states, Int. J. Mod. Phys. B **04**, 239 (1990).

[2] X.-G. Wen, Topological orders and Edge excitations in FQH states, Adv. Phys. **44**, 405 (1995).

[3] R. B. Laughlin, Anomalous Quantum Hall Effect: An Incompressible Quantum Fluid with Fractionally Charged Excitations, Phys. Rev. Lett. **50**, 1395 (1983).

[4] B. I. Halperin, Theory of the quantized Hall conductance, Helvetica Phys. Acta **56**, 75 (1983).

[5] F. D. M. Haldane, Model for a Quantum Hall Effect without Landau Levels: Condensed-Matter Realization of the"Parity Anomaly," Phys. Rev. Lett. **61**, 2015 (1988).

[6] C.-Z. Chang, J. Zhang, X. Feng, J. Shen, Z. Zhang, M. Guo, K. Li, Y. Ou, P. Wei, L.-L. Wang, Z.-Q. Ji, Y. Feng, S. Ji, X. Chen, J. Jia, X. Dai, Z. Fang, S.-C. Zhang, K. He, Y. Wang *et al.*, Experimental observation of the quantum anomalous Hall effect in a magnetic topological insulator, Science **340**, 167 (2013).

[7] G. Jotzu, M. Messer, R. Desbuquois, M. Lebrat, T. Uehlinger, D. Greif, and T. Esslinger, Experimental realization of the topological Haldane model with ultracold fermions, Nature (London) **515**, 237 (2014).

[8] J. Ge, Y. Liu, J. Li, H. Li, T. Luo, Y. Wu, Y. Xu, and J. Wang, High-Chern-number and high-temperature quantum Hall effect without Landau levels, Natl. Sci. Rev. **7**, 1280 (2020).

[9] Z. Liu and E. J. Bergholtz, From fractional Chern insulators to Abelian and non-Abelian fractional quantum Hall states: Adiabatic continuity and orbital entanglement spectrum, Phys. Rev. B **87**, 035306 (2013).

[10] T. Scaffidi and G. Möller, Adiabatic Continuation of Fractional Chern Insulators to Fractional Quantum Hall States, Phys. Rev. Lett. **109**, 246805 (2012).

[11] Y.-H. Wu, J. K. Jain, and K. Sun, Adiabatic continuity between Hofstadter and Chern insulator states, Phys. Rev. B **86**, 165129 (2012).

[12] A. S. Sørensen, E. Demler, and M. D. Lukin, Fractional Quantum Hall States of Atoms in Optical Lattices, Phys. Rev. Lett. **94**, 086803 (2005).

[13] R. N. Palmer and D. Jaksch, High-Field Fractional Quantum Hall Effect in Optical Lattices, Phys. Rev. Lett. **96**, 180407 (2006).

[14] M. Hafezi, A. S. Sørensen, E. Demler, and M. D. Lukin, Fractional quantum Hall effect in optical lattices, Phys. Rev. A **76**, 023613 (2007).

[15] T. Neupert, L. Santos, C. Chamon, and C. Mudry, Fractional Quantum Hall States at Zero Magnetic Field, Phys. Rev. Lett. **106**, 236804 (2011).

[16] K. Sun, Z. Gu, H. Katsura, and S. Das Sarma, Nearly Flatbands with Nontrivial Topology, Phys. Rev. Lett. **106**, 236803 (2011).

[17] E. Tang, J.-W. Mei, and X.-G. Wen, High-Temperature Fractional Quantum Hall States, Phys. Rev. Lett. **106**, 236802 (2011).

[18] D. N. Sheng, Z.-C. Gu, K. Sun, and L. Sheng, Fractional quantum Hall effect in the absence of Landau levels, Nat. Commun. **2**, 389 (2011).

[19] Y.-F. Wang, Z.-C. Gu, C.-D. Gong, and D. N. Sheng, Fractional Quantum Hall Effect of Hard-Core Bosons in Topological Flat Bands, Phys. Rev. Lett. **107**, 146803 (2011).

[20] N. Regnault and B. A. Bernevig, Fractional Chern Insulator, Phys. Rev. X **1**, 021014 (2011).

[21] D. J. Thouless, M. Kohmoto, M. P. Nightingale, and M. den Nijs, Quantized Hall Conductance in a Two-Dimensional Periodic Potential, Phys. Rev. Lett. **49**, 405 (1982).

[22] G. Möller and N. R. Cooper, Composite Fermion Theory for Bosonic Quantum Hall States on Lattices, Phys. Rev. Lett. **103**, 105303 (2009).

[23] G. Möller and N. R. Cooper, Fractional Chern Insulators in Harper-Hofstadter Bands with Higher Chern Number, Phys. Rev. Lett. **115**, 126401 (2015).

[24] F. Wang and Y. Ran, Nearly flat band with Chern number $C = 2$ on the dice lattice, Phys. Rev. B **84**, 241103(R) (2011).

[25] Y.-F. Wang, H. Yao, C.-D. Gong, and D. N. Sheng, Fractional quantum Hall effect in topological flat bands with Chern number two, Phys. Rev. B **86**, 201101(R) (2012).

[26] M. Trescher and E. J. Bergholtz, Flat bands with higher Chern number in pyrochlore slabs, Phys. Rev. B **86**, 241111(R) (2012).

[27] S. Yang, Z.-C. Gu, K. Sun, and S. Das Sarma, Topological flat band models with arbitrary Chern numbers, Phys. Rev. B **86**, 241112(R) (2012).

[28] M. Barkeshli and X.-L. Qi, Topological Nematic States and Non-Abelian Lattice Dislocations, Phys. Rev. X **2**, 031013 (2012).

[29] Z. Liu, E. J. Bergholtz, H. Fan, and A. M. Läuchli, Fractional Chern Insulators in Topological Flat Bands with Higher Chern Number, Phys. Rev. Lett. **109**, 186805 (2012).

[30] A. G. Grushin, T. Neupert, C. Chamon, and C. Mudry, Enhancing the stability of a fractional Chern insulator against competing phases, Phys. Rev. B **86**, 205125 (2012).

[31] D. Wang, Z. Liu, J. Cao, and H. Fan, Tunable Band topology Reflected by Fractional Quantum Hall States in Two-Dimensional Lattices, Phys. Rev. Lett. **111**, 186804 (2013).

[32] Y.-L. Wu, N. Regnault, and B. A. Bernevig, Bloch Model Wave Functions and Pseudopotentials for all Fractional Chern Insulators, Phys. Rev. Lett. **110**, 106802 (2013).

[33] Y.-L. Wu, N. Regnault, and B. A. Bernevig, Haldane statistics for fractional Chern insulators with an arbitrary Chern number, Phys. Rev. B **89**, 155113 (2014).

[34] A. Sterdyniak, C. Repellin, B. A. Bernevig, and N. Regnault, Series of Abelian and non-Abelian states in $c > 1$ fractional Chern insulators, Phys. Rev. B **87**, 205137 (2013).

[35] A. Kol and N. Read, Fractional quantum Hall effect in a periodic potential, Phys. Rev. B **48**, 8890 (1993).

[36] T. Senthil and M. Levin, Integer Quantum Hall Effect for Bosons, Phys. Rev. Lett. **110**, 046801 (2013).

[37] S. Furukawa and M. Ueda, Integer Quantum Hall State in Two-Component Bose Gases in a Synthetic Magnetic Field, Phys. Rev. Lett. **111**, 090401 (2013).

[38] Y.-H. Wu and J. K. Jain, Quantum Hall effect of two-component bosons at fractional and integral fillings, Phys. Rev. B **87**, 245123 (2013).

[39] N. Regnault and T. Senthil, Microscopic model for the boson integer quantum Hall effect, Phys. Rev. B **88**, 161106(R) (2013).

[40] S. D. Geraedts, C. Repellin, C. Wang, R. S. K. Mong, T. Senthil, and N. Regnault, Emergent particle-hole symmetry in spinful bosonic quantum Hall systems, Phys. Rev. B **96**, 075148 (2017).

[41] A. Sterdyniak, N. R. Cooper, and N. Regnault, Bosonic Integer Quantum Hall Effect in Optical Flux Lattices, Phys. Rev. Lett. **115**, 116802 (2015).

[42] Y.-C. He, S. Bhattacharjee, R. Moessner, and F. Pollmann, Bosonic Integer Quantum Hall Effect in an Interacting Lattice Model, Phys. Rev. Lett. **115**, 116803 (2015).

[43] T.-S. Zeng, W. Zhu, and D. N. Sheng, Bosonic integer quantum Hall states in topological bands with Chern number two, Phys. Rev. B **93**, 195121 (2016).

[44] Y.-C. He, F. Grusdt, A. Kaufman, M. Greiner, and A. Vishwanath, Realizing and adiabatically preparing bosonic integer and fractional quantum Hall states in optical lattices, Phys. Rev. B **96**, 201103(R) (2017).

[45] B. Andrews and G. Möller, Stability of fractional Chern insulators in the effective continuum limit of Harper-Hofstadter bands with Chern number $|C| > 1$, Phys. Rev. B **97**, 035159 (2018).

[46] E. M. Spanton, A. A. Zibrov, H. Zhou, T. Taniguchi, K. Watanabe, M. P. Zaletel, and A. F. Young, Observation of fractional Chern insulators in a van der Waals heterostructure, Science **360**, 62 (2018).

[47] S. R. White, Density Matrix Formulation for Quantum Renormalization Groups, Phys. Rev. Lett. **69**, 2863 (1992).

[48] I. P. McCulloch, Infinite size density matrix renormalization group, revisited, arXiv:0804.2509.

[49] A. G. Grushin, J. Motruk, M. P. Zaletel, and F. Pollmann, Characterization and stability of a fermionic $\nu = 1/3$ fractional Chern insulator, Phys. Rev. B **91**, 035136 (2015).

[50] Y.-C. He, D. N. Sheng, and Y. Chen, Obtaining topological degenerate ground states by the density matrix renormalization group, Phys. Rev. B **89**, 075110 (2014).

[51] M. P. Zaletel, R. S. K. Mong, and F. Pollmann, Flux insertion, entanglement, and quantized responses, J. Stat. Mech. (2014) P10007.

[52] W. Zhu, S. S. Gong, and D. N. Sheng, Chiral and critical spin liquids in a spin-$\frac{1}{2}$ kagome antiferromagnet, Phys. Rev. B **92**, 014424 (2015).

[53] H. Li and F. D. M. Haldane, Entanglement Spectrum as a Generalization of Entanglement Entropy: Identification of Topological Order in Non-Abelian Fractional Quantum Hall Effect States, Phys. Rev. Lett. **101**, 010504 (2008).

[54] W.-W. Luo, A.-L. He, Y. Zhou, Y.-F. Wang, and C.-D. Gong, Quantum phase transitions in a $\nu = \frac{1}{2}$ bosonic fractional Chern insulator, Phys. Rev. B **102**, 155120 (2020).

[55] B. Jaworowski, N. Regnault, and Z. Liu, Characterization of quasiholes in two-component fractional quantum Hall states and fractional Chern insulators in $|C| = 2$ flat bands, Phys. Rev. B **99**, 045136 (2019).

[56] D. N. Sheng, X. Wan, E. H. Rezayi, K. Yang, R. N. Bhatt, and F. D. M. Haldane, Disorder-Driven Collapse of the Mobility Gap and Transition to an Insulator in the Fractional Quantum Hall Effect, Phys. Rev. Lett. **90**, 256802 (2003).

[57] B. Blok and X. G. Wen, Effective theories of the fractional quantum Hall effect at generic filling fractions, Phys. Rev. B **42**, 8133 (1990).

[58] X. G. Wen and A. Zee, Shift and Spin Vector: New Topological Quantum Numbers for the Hall Fluids, Phys. Rev. Lett. **69**, 953 (1992).

[59] W. Zhu, Z. Liu, F. D. M. Haldane, and D. N. Sheng, Fractional quantum Hall bilayers at half filling: Tunneling-driven non-Abelian phase, Phys. Rev. B **94**, 245147 (2016).

[60] S. Furukawa and M. Ueda, Quantum Hall states in rapidly rotating two-component Bose gases, Phys. Rev. A **86**, 031604(R) (2012).

[61] Y.-F. Wang, H. Yao, Z.-C. Gu, C.-D. Gong, and D. N. Sheng, Non-Abelian Quantum Hall Effect in Topological Flat Bands, Phys. Rev. Lett. **108**, 126805 (2012).

[62] T.-S. Zeng, D. N. Sheng, and W. Zhu, Continuous phase transition between bosonic integer quantum Hall liquid and a trivial insulator: Evidence for deconfined quantum criticality, Phys. Rev. B **101**, 035138 (2020).

[63] W. Pan, W. Kang, M. P. Lilly, J. L. Reno, K. W. Baldwin, K. W. West, L. N. Pfeiffer, and D. C. Tsui, Particle-Hole Symmetry and the Fractional Quantum Hall Effect in the Lowest Landau Level, Phys. Rev. Lett. **124**, 156801 (2020).

[64] L. Schoonderwoerd, F. Pollmann, and G. Möller, Interaction-driven plateau transition between integer and fractional Chern Insulators, arXiv:1908.00988.